Austenite Grain Coarsening Under the Influence of Niobium Carbonitrides

David San Martín, Francisca G. Caballero, Carlos Capdevila and Carlos García de Andrés*

Solid-Solid Phase Transformations Group (GITFES), Department of Physical Metallurgy,
Centro Nacional de Investigaciones Metalúrgicas (CENIM), CSIC, Av. Gregorio del Amo 8, 28040, Madrid, Spain

This work investigates grain growth behaviour under the influence of pinning carbonitrides in a niobium microalloyed steel. The effect of temperature and heating rate on the grain size is studied. The grain coarsening temperature is determined as a function of the heating rate. It is found that unpinning by precipitates occurs around 40–70 K below the temperature of complete dissolution of carbonitrides. It has been found that experimental results are best described assuming a random distribution of carbonitrides in the matrix and niobium volume diffusion as the rate controlling process for the coarsening of precipitates. Austenite grain growth is explained theoretically taking as a basis the model proposed by *Zener*, which has been adapted for non-equilibrium kinetics, taking into account the experimental evidence that during a continuous heating, the amount of microalloyed element in solid solution is altered and different from that predicted by the solubility product.

1. Introduction

The driving force for grain growth results from the decrease in free energy of the system. The grain boundary area is the main source of energy for grain growth process; therefore, the system will evolve to reduce its grain boundary area.[1] Larger grains will grow at the expense of the smaller ones. Microalloying elements like vanadium, niobium and titanium have been employed in the past two decades to produce fine precipitation in the matrix. The austenite grain boundaries and dislocations are pinned by these precipitates, inhibiting their movement during the thermomechanical processing of steels.[2] This pinning force is governed by the thermodynamic stability of second-phase precipitates in austenite.[3–5] The temperature at which the equilibrium existing between driving forces for grain growth and pinning is broken, is defined as the grain coarsening temperature. At this temperature abnormal grain growth begins and a non-uniform grain microstructure is obtained.[6]

Austenite is the parent of the other microstructures, not only from the viewpoint that the other structures come from its decomposition, but also that it provides the framework for some of their characteristics. Shape and size of the austenite grain will determine the rates of transformation through points of nucleation and paths for transformation. The understanding of the grain coarsening behaviour is essential for predicting final mechanical properties of steels. In this sense a uniform fine-grained microstructure is very important. Therefore, due to its importance, the experimental determination and accurate theoretical prediction of the prior austenite grain size (*PAGS*) under the influence of pinning precipitates and the determination of the grain coarsening temperature becomes of the greatest importance in metallurgical studies.[7–12]

Zener[13] was the first to obtain a quantitative theoretical expression to evaluate the influence of precipitate inhibiting effect on grain boundary motion. This model balances the force for grain growth that arises from the decrease in grain boundary area per unit volume, against the pinning force

caused by precipitates present in the matrix. Other authors[14–22] have given several expressions since the seminal work by Zener, most of which incorporate Zener's ideas in some way. According to these expressions, depending on the size, the amount and distribution of precipitates in the matrix, the grain growth rate and the *3DPAGS* will be greatly affected. Although these models are based on a number of physical and geometric assumptions that differ among the models, all of them can be generalized using the following general equation,

$$D_{\mathrm{crit}} = \phi \frac{r}{f^n} \tag{1}$$

Where $\bar{D}_{\mathrm{crit}}$ is the average critical 3-D prior austenite grain size (*3DPAGS*) of the microstructure in the presence of a volume fraction of precipitates, f, that have a mean radius, r. The value of ϕ depends on factors such as the geometry of precipitates and austenite grains, or coherency between precipitate and matrix. This factor is usually considered as constant for a given steel. The value of n depends on the distribution of precipitates in the matrix. The assumption of random distribution leads to $n = 1$ (Zener original model), whereas preferential distribution of precipitates at grain boundaries leads to $n < 1$.[23]

The present article describes the austenite grain growth during a continuous heating at different rates in a niobium microalloyed steel. It will be discussed about the randomness of the distribution of carbonitrides in the matrix and whether volume diffusion or grain boundary diffusion of niobium is the rate controlling process for the coarsening of precipitates. A set of expressions is proposed to describe the austenite growth kinetics under the influence of pinning precipitates during a continuous heating at a constant rate.

2. Materials and Experimental Procedure

A low-carbon niobium microalloyed steel has been studied. Its chemical composition is listed in Table 1.

Cylindrical samples of 3 mm in diameter and 12 mm in length were used to reveal grain boundaries by the thermal etching method.[24,25] For this purpose, a surface 2 mm in

---

D. S. Martín, F. G. Caballero, C. Capdevila and C. G. d. Andrés

Table 1 Chemical composition (mass%).

C	Mn	Si	S	P	Nb	Cu	Cr	Ni	Mo	Al	N
0.11	1.47	0.27	0.013	0.015	0.031	0.011	0.03	0.03	0.006	0.039	0.0051

Table 2 Heating rates and austenitization temperatures.

Heating rate, HR/Ks^{-1}	Austenitization temperature, $T\gamma$/K
0.05, 0.5, 5	1183, 1223, 1273, 1323, 1373, 1423, 1473, 1523

width was generated along the longitudinal axis of samples by polishing and finishing with 1 μm diamond paste. Later on, these samples were austenitized in vacuum (>1 Pa) at different heating rates (*HR*) and at temperatures ranging from 1183 to 1523 K (*T*$_\gamma$). Subsequently samples were cooled down to room temperature at 1 K/s. In Table 2, heating rates and austenization temperatures studied are shown. These samples do not require metallographic preparation after heat treatment, and the prior austenite grain boundaries are revealed without chemical etching.

The average austenite grain size was measured using an image analyser. Pictures of the prior austenite microstructure were acquired and processed in order to generate a binary image in which prior austenite grain boundaries were shown in black. From this binary images the average area of austenite grains in 2-D, $\bar{A}$, was obtained.

In this work it will be considered that the three dimensional prior austenite grains can be represented as tetrakaidecahedrons. This polyhedron satisfies the space-filling and surface tension requirements. Hull and Houk[26] used a wire frame model of this polyhedron to get the distribution of areas of intersection with a given reference plane. They found that the mean, $\bar{A}$, and maximum, A_{max}, areas intersected could be related through the equation $\bar{A}/A_{max} = 0.546$. Taking into account that the distance between square faces of a tetrakaidecahedron can be written as $\bar{D} = 1.069\sqrt{A_{max}}$, a value for the average 3-D prior austenite grain size (*3DPAGS*) can be given,

$$\bar{D} = 1.447\sqrt{\bar{A}}. \tag{2}$$

A two-step extraction carbon replica method has been used to examine and identify precipitates present in the austenite grain boundaries.[27–30] In a first stage, triacetylcellulose thin films, which can be easily pasted onto the specimen surface with methyl acetate and then stripped off, are obtained. The second step consists in evaporation of carbon onto the plastic film in a high vacuum chamber. Carbon replicas obtained using this method where examined using a Jeol Jem 2010 TEM, at an operating voltage of 200 kV, with an energy dispersive spectroscopic (EDS) analyser Oxford Inca.

3. Results and Discussion

3.1 Evolution of the austenite grains with temperature and heating rate

Figure 1 shows the evolution of the *3DPAGS* during a continuous heating at 0.05, 0.5 and 5 K/s. Figure 2 shows the prior austenite microstructure formed after heating the sample to three different temperatures at a rate of 5 K/s.

Carbon replicas showed that in the present steel, niobium carbonitrides were precipitated in the matrix (Fig. 3). 'Cu' peaks in the EDS spectrum corresponds to the copper mesh that supports the replica. The average radius for carbonitrides measured from carbon replicas just above Ac_3 temperature was $r_0 = 0.01 \pm 0.004$ μm. Ac_3 is the temperature at which the process of austenitization is completed and it was experimentally determined for this steel at 1168 ± 3 K.[31]
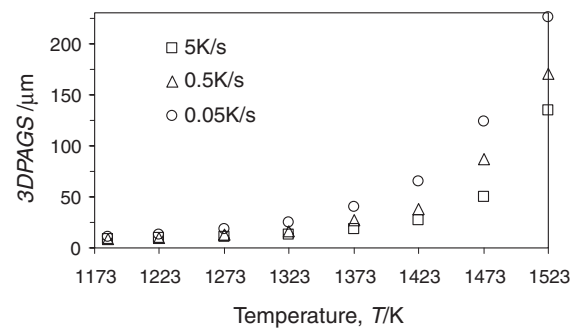

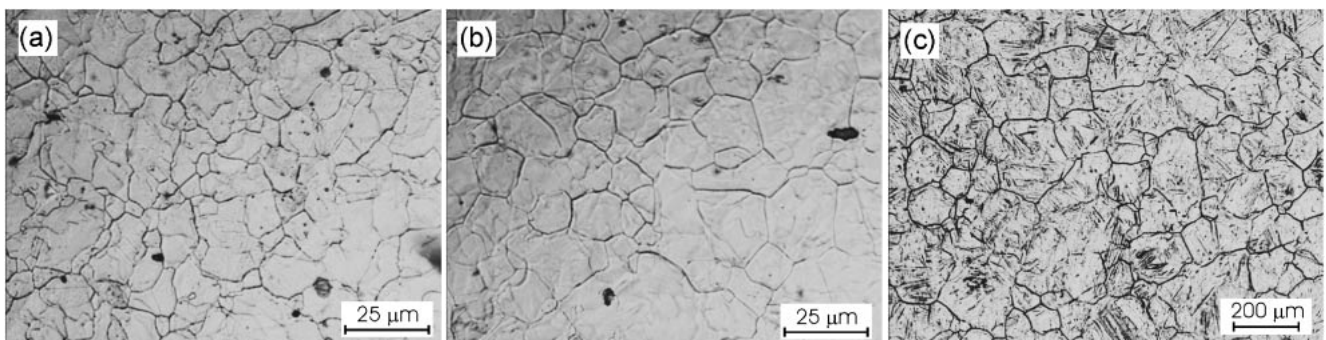Fig. 1 Evolution of the 3-D prior austenite grain size (*3DPAGS*) for three different heating rates.

Fig. 2 Prior austenite microstructure obtained after heating at 5 K/s; a) 1323 K, b) 1423 K and c) 1523 K.
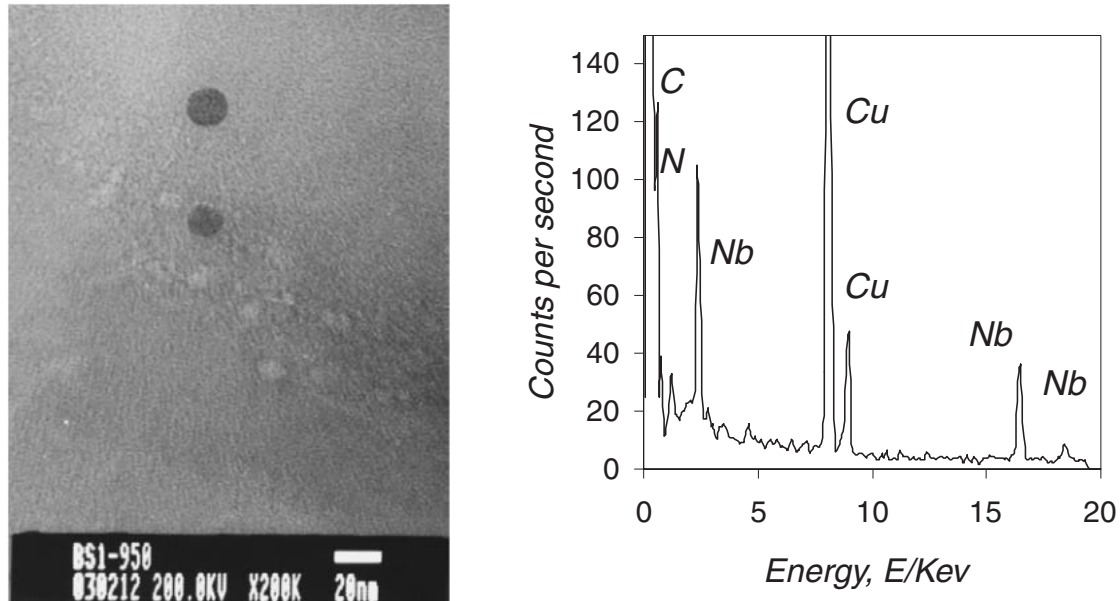
Fig. 3 Niobium carbonitride precipitated in the matrix.

It is well known that the *3DPAGS* in plain carbon steels increases exponentially with temperature.[4] However, in microalloyed steels is usual to observe two-step grain growth.[4,6,32,33] The sluggish grain growth in the lower range of temperatures (first step) is associated with the existence of precipitates that pin the boundaries, inhibiting their movement. As temperature is raised, several precipitates dissolve while others coarsen. Thus, some grain boundaries are free to move and the average *3DPAGS* of the microstructure will grow.

In microalloyed steels, although the limits between both steps of growth are not clearly divorced, the grain coarsening temperature (T_{GC}) is usually referred to as the temperature that separates both steps of growth.[6,34] The determination of this parameter is very important because differentiates a region of fine grains from a region where coarse grains are more likely to be found.

In Fig. 4 the T_{GC} measured by Palmiere *et al.*[34] and Cuddy and Raley[6] against niobium content of the steel has been
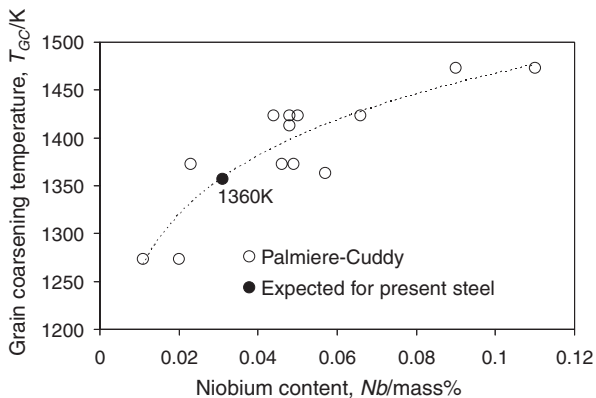

Fig. 4 Evolution of the grain coarsening temperature, T_{GC}, with niobium content of the steel (experimental data from the work of Palmiere *et al.*[33] and Cuddy *et al.*[6]).

represented. Data corresponding to steels from these authors have similar amount of carbon equivalent $C_{eq} = C + (12/14)N = 0.07$–$0.09\%$ and were obtained after heating for 30 minutes at the corresponding austenitizing temperature. C and N in this formula represent the carbon and nitrogen content in mass-%, respectively. From this figure, it seems to be a tendency to have a higher T_{GC} the higher the *Nb* content in the steel, as long as sufficient C_{eq} content is available to form more carbonitrides. According to this figure, it would be expected that $T_{GC} \approx 1360$ K (full circle in Fig. 4) in the steel studied in the present work under equilibrium condition. Since $\alpha \rightarrow \gamma$ transformation temperature (Ac_3) at 0.05 K/s are very close to those under equilibrium (Ae_3),[35,36] it has been considered in this work that heating rate of 0.05 K/s can reproduce equilibrium conditions. Bearing in mind such value of 1360 K for T_{GC}, it can be seen from Fig. 5(a) that fitting by two exponential functions of the form $k \exp(-q/T)$ is the best fit possible for data of Fig. 1. In this sense, it can be seen in Fig. 5(b) that fitting the experimental points by one exponential function is in less agreement than fitting with two functions. This result shows that grain growth during a continuous heating occurs in two steps rather than one.

In order to determine T_{GC} as a function of heating rate, it has been considered that the T_{GC} is that at which the exponential functions corresponding to each step intersect. In Fig. 6 the points of intersection between exponential functions corresponding to each step and heating rate are shown in detail. Results obtained are listed in Table 3.

From this table several conclusions can be drawn. First, T_{GC} lays around 40–70 K below the temperature of complete dissolution of carbonitrides (T_{DISS}), later calculated for this steel. Grain boundary unpinning requires that the precipitates dissolve and grow only to an extent at which the pinning force falls below a critical value and this happens well below T_{DISS}. This result is in agreement with the experimental work of Palmiere *et al.*,[34] Cuddy and Raley[6] and Gladman and
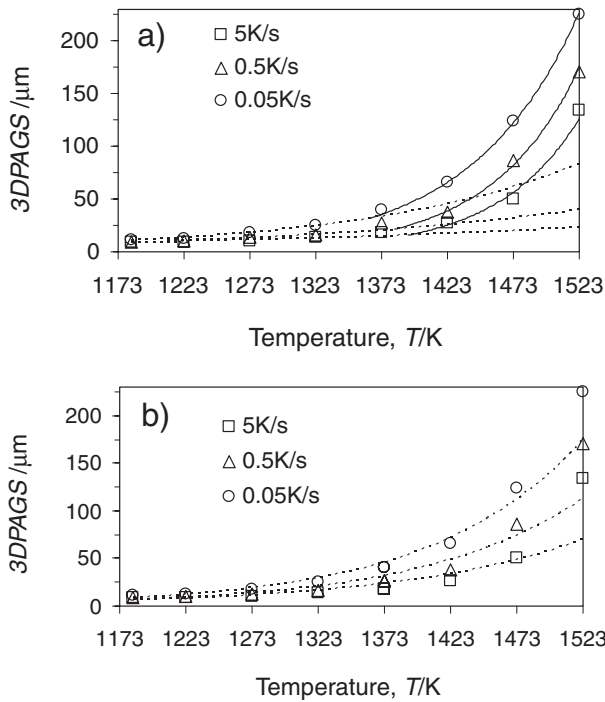
Fig. 5 Fitting of the experimental autenite grain size evolution; a) two exponential function and b) one exponential function.

Fig. 6 Determination of the grain coarsening temperature.

Table 3 Grain coarsening temperatures (T_{GC}) and corresponding 3-D prior austenite grain size (*3DPAGS*).

Heating rate, HR/Ks^{-1}	Grain coarsening temperature, T_{GC}/K	3-D prior austenite grain size, *3DPAGS*/μm
0.05	1363	32
0.5	1385	22
5	1393	15

Pickering.[3] Second, the faster the heating rate, the higher the grain coarsening temperature. This is due to the fact that with high heating rates, equilibrium conditions are not attained. Non-equilibrium leads to a decrease in the rate of dissolution and coarsening of precipitates. Finally, the faster the heating rate, the lower the *3DPAGS* at which grain coarsening starts.

3.2 Evolution of the volume fraction of niobium carbonitrides

At sufficiently high heating temperatures, the niobium carbonitrides precipitated in the matrix become unstable. Dissolution of some of the carbonitrides begins in order to reach the equilibrium amount of niobium in solid solution in austenite, as predicted by the solubility product of the niobium carbonitride,[34] at the corresponding temperature,

$$Log Ks = Log[Nb][C + (12/14)N] = 2.26 - (6770/T) \quad (3)$$

Where Nb, C and N refer to niobium, carbon and nitrogen in solid solution in austenite, respectively, in mass-%; Ks is the solubility product, and T is temperature in K.

As temperature is increased, more carbonitrides will dissolve and the volume fraction of these precipitates will decrease until the T_{DISS} is attained. At this temperature all precipitates will be dissolved and all the Nb, C and N will be in solid solution in the austenitic matrix. According to eq. (3), for the present steel, $T_{DISS} = 1437$ K. This temperature is very similar to that predicted by MTDATA software[37] (1423 K).

Considering mass balance of niobium and carbon equivalent, $Nb = Nb^P + [Nb]$ and $C_{eq} = C_{eq}^P + [C_{eq}]$, and the stoichiometric relation, $C_{eq}^P/Nb^P = A_C/A_{Nb}$, the following expression can be obtained for the amount of niobium precipitated as carbonitrides (eq. 4) and niobium in solid solution in equilibrium with austenite (eq. 5),

$$Nb^P = \frac{[(A_C Nb/A_{Nb}) + C_{eq}] - \{[(A_C Nb/A_{Nb}) + C_{eq}]^2 - (4A_C/A_N b)(C_{eq}Nb - Ks)\}^{1/2}}{2A_C/A_{Nb}} \quad (4)$$

$$[Nb] = Nb - Nb^P \quad (5)$$

Where Nb refers to the nominal composition of the steel; Nb^P and C_{eq}^P are the niobium and carbon equivalent content precipitated as carbonitrides, respectively; and A_C (12.01) and A_{Nb} (92.91) are the atomic weight of carbon and niobium, respectively.

Approximating the total volume of the system as the sum of that of austenite and niobium carbonitrides, an expression for the volume fraction of carbonitrides can be achieved,

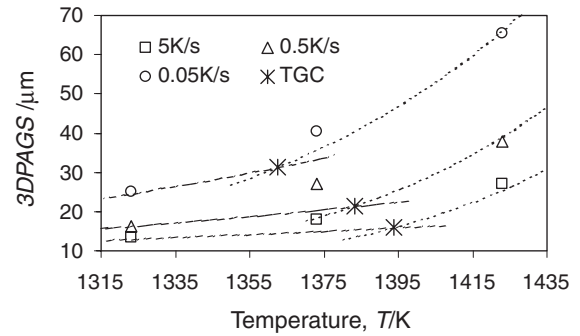$$f = \left[\frac{\rho_{NbCN}}{\rho_{Fe}^\gamma} \frac{m_{Fe}^\gamma}{m_{NbCN}} + 1\right]^{-1} \quad (6)$$

Where ρ_{NbCN}, m_{NbCN}, ρ_{Fe}^γ and m_{Fe}^γ are the density and mass of niobium carbonitrides and austenite, respectively. Finally, m_{NbCN} and m_{Fe}^γ can be written as a function of Nb^P,

$$m_{NbCN} = (Nb^P/100)(A_{Nb} + A_C)/A_{Nb} \quad (7)$$

$$m_{Fe}^\gamma = 1 - m_{NbCN} \quad (8)$$

In Fig. 7 the evolution of the amount of niobium in solid solution, $[Nb]$, and equilibrium volume fraction of niobium carbonitrides, f, have been represented as a function of temperature, eqs. (5) and (6), respectively. As it is shown in this figure, for $T > 1437$ K, no carbonitride will remain precipitated in the austenitic matrix.
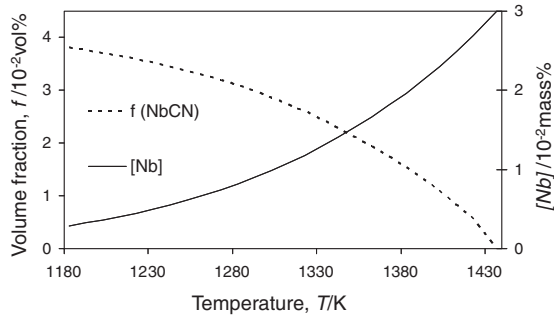
Fig. 7 Evolution of the equilibrium volume fraction of carbonitrides and the amount of niobium in solid solution at each heating temperature.

3.3 Evolution of the radius of niobium carbonitrides

On the other hand, some experimental works have shown that during heating, precipitates that remain undissolved in the matrix have a tendency to coarsen at the expense of the smaller ones.[3,4,38] The driving force for this process is provided by the consequent reduction in the total interfacial energy. These authors[3,4,38] experimentally showed that the higher the heating temperature, the coarser the niobium carbonitrides were, although less volume fraction of them were precipitated in the matrix.

Other authors[39] have observed that for heating temperatures lower than the T_{DISS}, coarsening of precipitates was taking place; while for heating temperatures higher than T_{DISS}, only dissolution occurred.

Depending on the rate controlling process, the law that describes the coarsening of carbonitrides varies. The diffusivity of niobium is much lower than the diffusivity of carbon or nitrogen in austenite; hence, niobium diffusion is supposed to be the rate controlling process during ripening of carbonitrides. If most precipitates are located preferentially at grain boundaries, it is expected that during coarsening, most of the niobium in solid solution will diffuse along grain boundaries. In this case, according to Ardell[40] the variation of mean radius of grain boundary precipitates with time is described by the following expression,

$$r^3 \frac{dr}{dt} = \frac{2\sigma[Nb]\delta D_{GB}V_m}{3\nu GRT} \qquad (9)$$

Where r is the radius of carbonitrides in microns, T is the absolute temperature, t is time in seconds, σ is the interfacial energy per unit area between precipitate and matrix, δ is the width of the grain boundary, V_m is the molar volume of carbonitrides, D_{GB} is the coefficient of niobium diffusion in grain boundaries, $[Nb]$ is the amount of niobium, in mass-%, in solid solution in equilibrium with the austenite matrix, ν is a parameter determined by Ardell[40] that varies rapidly for small values of f, and R is the universal gas constant. G is a geometrical constant characteristic of a given system.[40]

$$G = \left[\frac{2}{3} - \frac{\gamma}{2\sigma} + \frac{1}{3}\left(\frac{\gamma}{2\sigma}\right)^3\right] \bigg/ \left[1 - \left(\frac{\gamma}{2\sigma}\right)^2\right]^2 \qquad (10)$$

Where γ is the grain boundary energy per unit area.

During a continuous heating, the heating curve can be expressed as a serie of isothermal steps that occur at consecutively increasing temperatures. In this sense, the total increase in the radius of carbonitrides during heating can be computed as the sum of the partial contributions at each heating temperature (step). The heating time at each step, can be expressed as a function of the heating rate $dt = dT/\theta$, where θ is the heating rate and dT is the increment in temperature between two successive steps. In the limit where $dT \rightarrow 0$, the sum of consecutive steps can be simplified integrating in the whole range of temperatures $[Ac_3, T]$. Therefore, the radius of niobium carbonitrides during heating can be written as,

$$r^4 = r_0^4 + \frac{8\sigma\delta V_m}{3GR\theta}\int_{A_{c3}}^T \frac{[Nb]D_{GB}}{\nu T}\,dT \qquad (11)$$

where r_0 is the radius of precipitates at the end of austenite formation.

On the other hand, if precipitates are distributed in austenite at random, due to the low volume fraction of the sample occupied by the grain boundaries, the number of precipitates present in the matrix will be higher than those located at grain boundaries. In this case, most of niobium in solid solution will diffuse through the volume of the austenitic matrix in order to contribute to the coarsening of niobium carbonitrides located at grain boundaries. In this case, according to the theory by Lifshitz and Slyozov,[41] precipitate coarsening is controlled by niobium volume diffusion, an equivalent expression to eq. (11) can be obtained,

$$r^3 = r_0^3 + (4\sigma V_m/9R\theta)\int_{A_{c3}}^T \frac{[Nb]D_V}{T}\,dT \qquad (12)$$

Where D_V is the coefficient of niobium volume diffusion. The other parameters in eq. (12) have been defined previously.

In Fig. 8(a) and Fig. 8(b) the evolution of the radius of niobium carbonitrides with temperature and heating rate has been represented as predicted by eqs. (11) and (12), respectively. The values used for different physical parameters, for the calculation of eqs. (10), (11) and (12), are listed in Table 4. The coefficient of niobium volume diffusion has been calculated following the data reported by Fridberg et al.[43] Moreover, according to Fridberg's work, it has been considered that the activation energy for niobium grain boundary diffusion is $Q_{GB} = Q_V/1.8$, where Q_V is the activation energy for niobium volume diffusion.

As it would be expected, Fig. 8 shows that the coarsening of carbonitrides controlled by niobium grain boundary diffusion is much faster than coarsening governed by niobium volume diffusion.

3.4 Theory of grain growth under the influence of pinning carbonitrides during a continuous heating

As it was pointed out in the introduction of this work, all models concerning the growth of grains under the influence of a dispersed second phase can be generalized using eq. (1). According to this equation, the limiting grain size critically depends on the assumptions regarding the randomness of the boundary particle correlations. Following the works by Doherty et al.,[45] and Anand and Gurland,[46] if most of the particles were located at grain boundaries, eq. (1) should have the form,
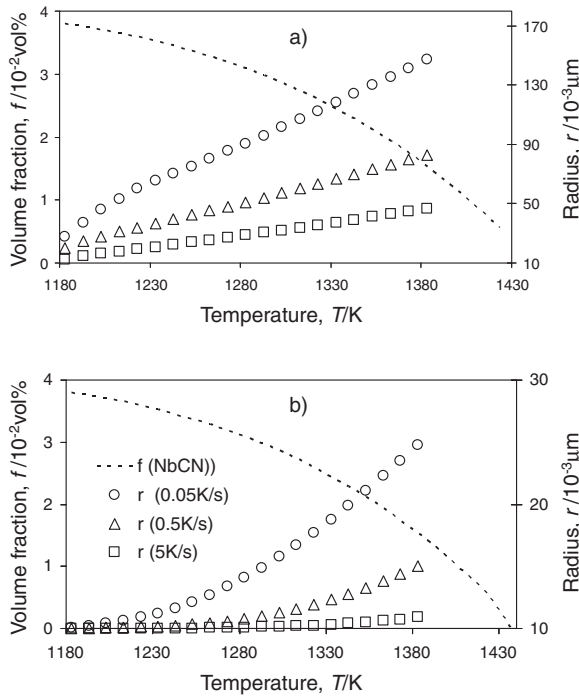
Fig. 8　Evolution of the radius of niobium carbonitrides with heating rate and temperature under two different assumptions: a) coarsening controlled by niobium grain boundary diffusion and b) controlled by niobium volume diffusion. Evolution of the equilibrium volume fraction of carbonitrides is also shown (dashed line).
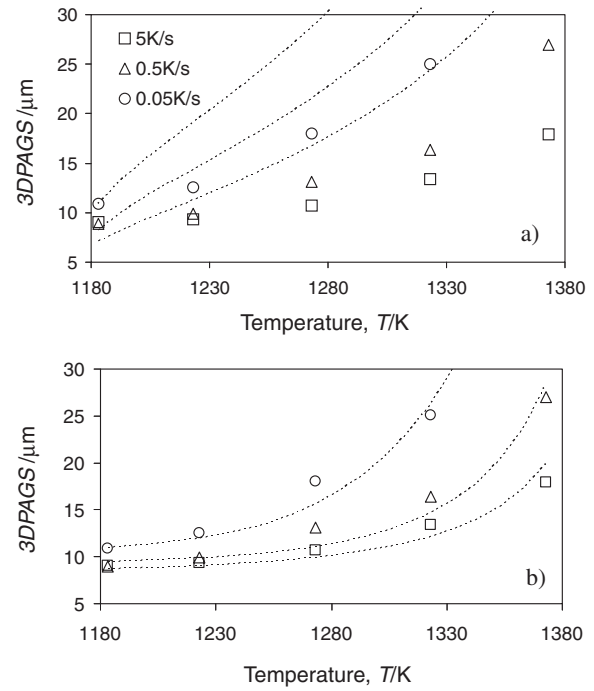

Fig. 9　Evolution of the experimental (open points) and theoretical (dot lines) values of $\bar{D}_{\text{crit}}$ during a continuous heating according to the predictions of two different models: a) most precipitates located at grain boundaries, coarsening of precipitates governed by niobium grain boundary diffusion; b) precipitates randomly located in the matrix, coarsening of precipitates mainly governed by niobium volume diffusion.

Table 4　Parameters used for the calculation of eqs. (11) and (12).

Parameter	Symbol	Value	Reference
Bulk diffusion of *Nb* in austenite	$D_{\text{V}}/\mu\text{m}^2\text{s}^{-1}$	$9.3 \times 10^8 \exp(-291966/RT)$	43
Grain boundary diffusion of *Nb* in austenite	$D_{\text{GB}}/\mu\text{m}^2\text{s}^{-1}$	$9.3 \times 10^8 \exp(-162203/RT)$	43
Interfacial energy matrix/precipitate	$\sigma/\text{J}\mu\text{m}^{-2}$	0.5×10^{-12}	42
Grain boundary energy	$\gamma/\text{J}\mu\text{m}^{-2}$	0.75×10^{-12}	44
Molar volume *NbCN*	$V_{\text{m}}/\mu\text{m}^3\text{mol}^{-1}$	1.28×10^{13}	42
Grain boundary width	$\delta/\mu\text{m}$	10^{-3}	44
Universal gas constant	$R/\text{JK}^{-1}\text{mol}^{-1}$	8.31	
Initial radius *NbCN*	$r_0/\mu\text{m}$	0.01 ± 0.004	

$$\bar{D}_{\text{crit}} = \phi \frac{r}{f^{1/2}} \qquad (13)$$

On the other hand, as originally proposed by Zener,[13] and also shown by several authors,[14,21] the assumption of random intersection between grain boundaries and second phase particles leads to $n = 1$ in eq. (1),

$$\bar{D}_{\text{crit}} = \phi \frac{r}{f} \qquad (14)$$

Therefore, according to eqs. (13) and (14) depending on the distribution of precipitates in the matrix, two different models should be used in the calculations. If precipitates are mainly located at grain boundaries, eqs. (6), (11) and (13) would have to be applied. In this configuration, precipitates would coarsen due to the diffusion of niobium coming through the

grain boundaries because most of the precipitates would dissolve at grain boundaries, putting in solution niobium in these locations. By contrast, if precipitates are distributed randomly in the microstructure, eqs. (6), (12) and (14) have to be used. Most precipitates would be dissolving in the matrix and, therefore, niobium would be reaching precipitates mainly by volume diffusion through the matrix.

In Figs. 9a) b) results obtained using the two models have been represented. These results show that grain growth under the influence of precipitates that are pinning grain boundaries is best modelled assuming that precipitates are distributed at random in the microstructure and that the process controlling the coarsening of precipitates is the niobium volume diffusion. Figure 9a) shows that coarsening of precipitates due to grain boundary diffusion predicts much faster grain growth kinetics than the growth measured experimentally.

These results are in agreement with the results of other authors concerning the modelling of austenite grain growth under the influence of carbonitrides.[3,38,47–50] Consequently, eqs. (14) along with eqs. (6) and (12) are the ones that best describe the austenite grain growth under the influence of precipitates for the present steel.

In order to give a better description of the kinetics of austenite grain growth during a continuous heating, eq. (14) can be rewritten as,

$$\bar{D}_{\text{crit}} = \beta\left(\alpha\frac{r}{f}\right) \tag{15}$$

The value of β depends on factors such as the geometry of precipitates and austenite grains, or coherency between precipitate and matrix and is constant for a given steel. In this equation, when calculating theoretically the value of r/f, equilibrium conditions have been considered based on eq. (3). However, it can be expected that during a continuous heating, equilibrium conditions will not be attained. In this sense, parameter α gives an estimation of the effect of the non-equilibrium continuous heating on the value of r/f. It will be assumed that the equilibrium volume fraction of carbonitrides, f (eq. 6), and the equilibrium content of niobium in solid solution, $[Nb]$ (eq. 5), is reached at each austenitization temperature only for a heating rate of 0.05 K/ s. The eq. (15) is only valid for temperatures before the grain coarsening temperature (T_{GC}). Therefore, according to results in Table 3, for a heating rate of 0.05 K/s this equation is only valid for experimental values raging from 1183 K to 1323 K, while for 0.5 and 5 K/s is valid from 1183 to 1373 K.

Considering that β is constant with temperature and heating rate and that under equilibrium conditions (0.05 K/s), $\alpha = 1$; these two parameters are obtained from best fit possible between experimental and eq. (15). The best fit was already shown in Fig. 9b).

To obtain the value of β and α in an easy and direct way, experimental average critical *3DPAGS*, $\bar{D}_{\text{crit}}$, was represented against the calculated value of r/f for each heating temperature and in the range of temperatures mentioned before (Fig. 10). From the slope of the linear fits (dashed lines) of the points corresponding to each heating rate, parameters β and α have been deduced. Table 5 lists the values of β and α obtained. As it would be expected,
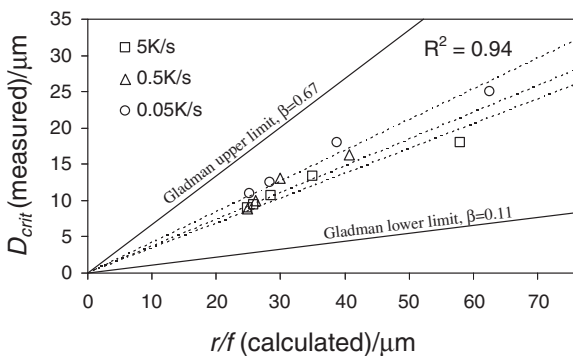

Fig. 10 Relationship between average critical *3DPAGS*, $\bar{D}_{\text{crit}}$, and r/f for the three heating rates (open circles, squares and triangles) compared with limits given by *Gladman*[3] (thick lines).

Table 5 Experimental β and α parameters ($R^2 = 0.94$).

Heating rate, HR/Ks^{-1}	α	β
0.05	1	0.44
0.5	0.86	0.44
5	0.80	0.44

Table 6 Value of β (eq. (15)) found in the literature.

Zener[13]	Hannerz[14]	Gladman[15]	Rios[17]	Ogino[18]
3.41	0.44	$(2.56)\pi[(1/4) - (1/3Z)]$*	0.43	0.33

*Z is the ratio of diameter of growing grains to matrix grains ($\sqrt{2} < Z < 2$). Since all the authors consider two-dimensional grain radius instead of three-dimensional diameter in their calculation, in this table, their values have been multiplied by a factor of '2.56' following the work of Hull and Houk,[23] $D_{\text{crit}}(3D) = 2.56R_{\text{crit}}(2D)$.

parameter α decreases as the heating rate increases. In this figure, the experimental values have been compared with limits given by Gladman theory[51] (thick lines). The value of β obtained is also similar to estimations predicted or measured by other authors (see Table 6).

Finally, from results shown above, the evolution of the pinning driving force of niobium carbonitrides with temperature for the heating rates studied can be calculated. The pinning driving force associated with niobium carbonitrides can be written as,

$$G_{\text{Z}} = k_1\gamma\frac{f}{r} \tag{16}$$

Where γ is the grain boundary energy and k_1 is a parameter dependent on the geometry of carbonitrides and coherency between precipitates and the matrix. On the other hand, the driving force for grain boundary migration is inversely proportional to the average *3DPAGS* ($\bar{D}$),

$$G_{\text{GG}} = k_2\frac{\gamma}{\bar{D}} \tag{17}$$

Where k_2 depends on the geometry of three dimensional austenite grains. When grain boundaries are pinned ($T < T_{\text{GC}}$), $G_{\text{Z}} = G_{\text{GG}}$ and $\bar{D}$ corresponds to $\bar{D}_{\text{crit}}$ in eq. (15). Thus, the following expression is achieved,

$$k_1 = k_2/\alpha\beta \tag{18}$$

Therefore, the pinning force (eq. (16)) can be rewritten as,

$$G_{\text{Z}} = \frac{k_2\gamma}{\alpha\beta}\frac{f}{r} = \frac{\eta}{\alpha}\frac{f}{r} \tag{19}$$

Where $\eta = k_2\gamma/\beta$. Assuming the geometry of prior austenite grains as tetrakaidecahedrons ($k_2 = 3.35$[52]) and taking $\gamma = 0.75 \times 10^{-12}$ J/μm,[44] it is found that $\eta = 6.0 \times 10^{-12}$ J/ μm^2. Figure 11 shows the evolution of the real pinning force, G_{Z}, given by eq. (17), with temperature for each heating rate. An increase in the heating rate affects the dissolution and coarsening kinetics of carbonitrides, delaying these processes and causing the grain boundary pinning to increase. Therefore, the higher the heating rate, the larger and finer distribution of carbonitrides is present in the microstructure.
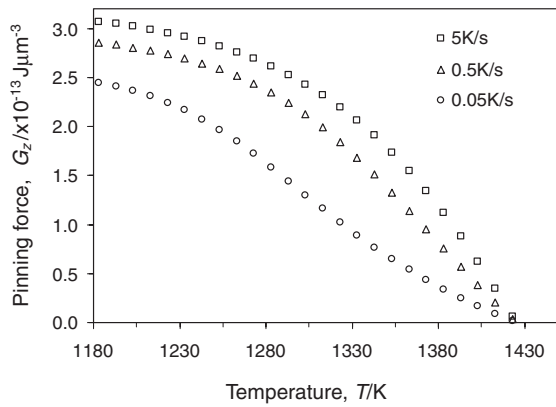
Fig. 11 Evolution of the pinning driving force due to niobium carbonitrides during a continuous heating as a function of the heating rate and temperature.

4. Conclusions

(1) The niobium microalloyed steel studied shows a two-stage grain growth during a continuous heating rather than one step continuous growth due to the existence of niobium carbonitrides precipitated in the matrix. The grain coarsening temperature (T_{GC}) has been obtained. It has been found that as the heating rate increases, T_{GC} temperature increases and the grain size at that temperature decreases. T_{GC} temperature lays around 40–70 K below the temperature of complete dissolution of carbonitrides (T_{DISS}).

(2) It has been found that austenite grain growth under the influence of niobium carbonitrides is best described under the assumption of random distribution of precipitates (Zener original model) and that coarsening of precipitates is mainly controlled by niobium volume diffusion. Based on the theory by Zener, a new expression has been proposed to describe the austenite grain coarsening under the influence of pinning precipitates during a continuous heating at a constant rate.

(3) An expression has been obtained to describe the pinning force exerted by a distribution of niobium carbonitrides during a continuous heating at different rates.

Acknowledgements

REFERENCES

1) H. V. Atkinson: Acta Metall. **36** (1988) 469–491.
2) N. T. Baker: *Future Developments of Metals and Ceramics*, edited by J. A. Charles, G. W. Greenwood and G. C. Smith, (Institute of Materials, London, 1992) pp. 75.
3) T. Gladman and F. B. Pickering: J. Iron Steel Inst. **205** (1967) 653–664.
4) R. Coladas, J. Masounave, G. Guérin and J.-P.Bailón: Met. Sci. **November** (1977) 509–516.
5) G. R. Speich, L. J. Cuddy, C. R. Gordon and A. J. DeArdo: *Phase Transformations in Ferrous Alloys*, A. R. Marder and J. I. Goldstein eds., (TMS-AIME, Warrendale, PA, 1984) pp. 341.
6) L. J. Cuddy and J. C. Raley: Metall. Trans. A **14** (1983) 1989–1995.
7) H. Ohtani, F. Terasaki and T. Kunitake: Trans. ISIJ **12** (1972) 118–127.
8) N. J. Petch: J. Iron Steel Inst. **174** (1953) 25–28.
9) A. Grange: Trans. Am. Soc. Met. **59** (1966) 26.
10) S. Kim, S. Lee and B. S. Lee: Mater. Sci. Eng. A **359** (2003) 198–209.
11) J. Kusiak and R. Kuziak: J. Mater. Process. Tech. **127** (2002) 115–121.
12) A. Di Schino, M. Barteri and J. M. Kenny: J. Mater. Sci. **38** (2003) 4725.
13) C. Zener, quoted by C. S. Smith: Trans. AIME **175** (1948) 15–51.
14) M. Hillert: Acta Metall **13** (1965) 227–238.
15) T. Gladman: Proc. R. Soc. **294A** (1966) 298.
16) N. A. Haroun and D. W. Budworth: J. Mater. Sci. **3** (1968) 326–328.
17) N. A. Haroun: J. Mater. Sci. **15** (1980) 2816.
18) P. Hellman and M. Hillert: Scand. J. Metall. **4** (1975) 211–219.
19) N. Ryum, O. Hunderi and E. Nes: Scr. Metall. **17** (1983) 1281.
20) E. Nes, N. Ryum and O. Hunderi: Acta Metall. **33** (1985) 11.
21) P. R. Rios: Acta Metall. **35** (1987) 2805–2814.
22) Y. Ogino: Tetsu-to-Hagané **57** (1971) 533.
23) Y. X. Liu and B. R. Patterson: Acta. Mater. **44** (1996) 4327–4335.
24) C. García de Andrés, M. J. Bartolomé, C. Capdevila, D. San Martín, F. G. Caballero and V. López: Mater. Charact. **46** (2001) 389–398.
25) C. García de Andrés, F. G. Caballero, C. Capdevila and D. San Martín: Mater. Charact. **4** (2003) 121–127.
26) F. C. Hull and W. J. Houk: J. Met. **April** (1953) 565–572.
27) G. R. Booker and J. Norbury: British J. Appl. Phys. **8** (1957) 109.
28) C. P. Scott, D. Chaleix, P. Barges and V. Rebischung: Scr. Mater. **47** (2002) 845–849.
29) S. G. Hong, H. J. Jun, K. B. Kang and C. G. Park: Scr. Mater. **48** (2003) 1201–1206.
30) A. Fukami: Jeol News **July** (1967) 5–7.
31) D. San Martín: *Modelización de la cinética de austenización y crecimiento de grano austenítico en aceros ferrítico-perlíticos*, PhD Thesis, (Universidad Complutense of Madrid, Spain, 2003) pp. 159.
32) F. Peñalba, C. García de Andrés, M. Carsí and F. Zapirain: J. Mater. Sci. **31** (1996) 3847–3852.
33) C. García de Andrés, C. Capdevila, F. G. Caballero and D. San Martín: J. Mater. Sci. **36** (2001) 565–571.
34) E. J. Palmiere, C. I. Garcia and A. J. DeArdo: Metall. Mater. Trans. A **25** (1994) 277–286.
35) K. W. Andrews: JISI **July** (1965) 721–727.
36) M. Atkins: *Atlas of Continuous Cooling Transformation Diagrams for Engineering Steels*, (British Steel Co., Sheffiled, United Kingdom, 1985) pp. 10–340.
37) H. Davies: *MTDATA* (National Physical Laboratory, Teddington, UK, 2003).
38) E. Anelli, M. Paolicchi and G. Quintiliani: Private Communication.
39) L. M. Cheng, E. B. Hawbolt and T. R. Meadowcroft: Can. Metall. Quart. **39** (2000) 73–86.
40) A. J. Ardell: Acta Metall. **20** (1972) 601–609.
41) I. M. Lifshitz and V. V. Slyozov: J. Phys. Chem. Solids **19** (1961) 35–50.
42) B. Dutta, E. Valdés and C. M. Sellars: Acta Metall. Mater. **40** (1992) 653.
43) J. Fridberg, L. E. Törndahl and M. Hillert: Jernkont. Ann. **153** (1969) 263–276.
44) H. S. Zurob, C. R. Hutchinson, Y. Brechet and G. Purdy: Acta Mater. **49** (2001) 4183–4190.
45) R. D. Doherty, D. J. Srolovitz, A. D. Rollet and M. P. Anderson: Scr. Metall. **21** (1987) 675–679.
46) L. Anand and J. Gurland: Metall. Trans. A **6A** (1975) 928.
47) T. Siwecki, S. Zajac and Goran Engberg: Proceedings of the 37th Mechanical Working and Steel Processing Conference (1996) 721–734.
48) T. Gladman: Iron Steelmak. **16** (1989) 241–245.
49) N. E. Hannerz and F. de Kazinczy: J. Iron Steel Inst. **May** (1970) 475–481.
50) P. A. Manohar, D. P. Dunne, T. Chandra and C. R. Killmore: ISIJ Int. **36** (1996) 194–200.
51) T. Gladman: *The Physical Metallurgy of Microalloyed Steels*, (The Institute of Materials, London, UK, 1997) pp. 176.
52) J. W. Cahn: Acta Metall. **4** (1956) 449–459.